Original Article

Circ_0087960 stabilizes KDM5B by reducing SKP2 mediated ubiquitination degradation and promotes osteogenic differentiation in periodontal ligament stem cells

Yinchen Liu, Yanbin Zhou*

Department of Stomatology, The Second Xiangya Hospital of Central South University, Changsha 410011, Hunan Province, PR China

A B S T R A C T

Background: Periodontitis is a common chronic oral disease among the world. Periodontal ligament stem cells (PDLSCs) has been proved to be a promising tool for the treatment of periodontitis due to their capability of generating periodontal tissues. Circ_0087960 and KDM5B have been shown to participate in the process of osteogenic differentiation with unclear function and mechanism.
Methods: Circ_0087960 and KDM5B expressions were detected during the osteogenic induction of PDLSCs. The functions of circ_0087960 and KDM5B were validated by manipulating their expression with shRNA. ChIP and luciferase reporter assays were used to prove the KDM5B-based osteogenic gene regulation. Co-IP assay was used to determine the interaction between SKP2 and KDM5B. In vivo ubiquitination assay was used to test the modification of KDM5B by SKP2. RNA pull-down was used to demonstrate the interaction between circ_0087960 and KDM5B.
Results: Circ_0087960 and KDM5B were found to be upregulated in the osteogenic differentiation of PDLSCs and promote the expression of related genes. KDM5B could directly bind and promote the expression of Runx2, ALP and OCN. KDM5B protein level in PDLSCs was controlled by SKP2-mediated protein ubiquitination and degradation. Circ_0087960 was identified to bind to KDM5B protein and protect it against SKP2-induced protein degradation, leading to the upregulation of osteogenic genes.
Conclusion: Circ_0087960 and KDM5B could be applied as promising therapeutic methods to stimulate the osteogenic differentiation of PDLSCs, expanding their capability in the treatment of periodontitis.
© 2022, The Japanese Society for Regenerative Medicine. Production and hosting by Elsevier B.V. This is an open access article under the CC BY-NC-ND license (http://creativecommons.org/licenses/by-nc-nd/4.0/).

1. Introduction

As one of the most frequent chronic oral diseases, Periodontitis leads to the deficiency of structures, including periodontal ligament, alveolar bone and cementum, that support to the teeth [1]. Limited effective treatments are available for periodontitis due to the loss of regeneration ability for periodontal tissue [2]. Recently, a diverse group of mesenchymal stem cells (MSCs) derived from dental stem cells has attracted attention due to their potential to differentiate into various cell types [3]. Periodontal ligament stem cells (PDLSCs) belong to those dental stem cells with reported capability as a therapeutic method for periodontal diseases, as well as other diseases related to bone or tissue deficiencies [4]. Most significantly, PDLSCs has been shown to maintain a unique feature to generate periodontal tissues, acting as an promising candidate to deal with the loss of periodontal bone [5,6].

Circular RNAs (circRNAs) are a family of noncoding RNA characterized by a cyclic covalent structure without 5' cap and 3' tail, which is more stable compared to linear RNA [7—9]. The functions of circRNAs have been widely explored in different models and cell types. In particular, circRNA CDR1as has been reported to regulate osteogenic differentiation of PDLSCs [10]. Moreover, a detailed research has been conducted to investigate the expression profile of circRNAs in PDLSCs and circ_0087960 is demonstrated to be upregulated after osteogenic differentiation [11]. However, the function of circ_0087960 in PDLSCs differentiation remains unclear.

* Corresponding author. Department of Stomatology, The Second Xiangya Hospital of Central South University, No.139, Middle Renmin Road, Changsha 410011, Hunan Province, PR China.
E-mail address: zhouyb@csu.edu.cn (Y. Zhou).

KDM5B is a member of the family of Jumonji-Homology Domain demethylase that acts as a suppressor for target genes by catalyzing the removal of the H3K4me3 mark [12]. KDM5B has been reported to form multi-enzymatic complexes that regulate transcriptional repression associated with histone deacetylases and lysine methylases [13,14]. Meanwhile, it has been shown that KDM5B controls the osteogenic lineages differentiation of mesenchymal cells by regulating the level of Runx2 [15], indicating the potential role of KDM5B in osteogenic differentiation of PDLSCs. Interestingly, the S-phase kinase associated protein-2 (SKP2), which is an E3 ligase and a component of SKP2-SCF complex, has been identified to regulate KDM5B level via ubiquitin-mediated protein degradation in prostate cancer cells [16]. Meanwhile, circ_0087960 is predicted to interact with KDM5B protein by RPIseq database, suggesting the crosstalk among circ_0087960, KDM5B and SKP2 in regulating osteogenic differentiation.

In this work, we demonstrated that circ_0087960 and KDM5B were upregulated during the osteogenic differentiation process of PDLSCs. KDM5B was proved to promote the expression of osteogenic related genes transcriptionally. Meanwhile, SKP2 was found to enhance the protein degradation of KDM5B in an ubiquitin-dependent manner. Moreover, circ_0087960 was identified to bind to KDM5B protein and protect it from SKP2-mediated degradation, resulting into a restore of downstream target genes and stimulating PDLSCs differentiation. Our study discovered the molecular mechanism and function of circ_0087960 and KDM5B in the osteogenic differentiation process of PDLSCs and facilitated the application of PDLSCs into the treatment of periodontitis.

2. Methods and materials

2.1. Isolation and culture of PDLSCs

The work was reviewed and permitted by the Medical Ethics Committee of Department of Stomatology, The Second Xiangya Hospital of Central South University. All the dental tissues used in this study were from patients signed the informed consent and underwent oral surgeries at the Department of Stomatology, The Second Xiangya Hospital of Central South University hospital. The teeth without healthy issues were extracted and periodontal tissues were collected from the surface of middle third of the tooth. The tissues were then incubated in a solution with dispase (4 mg/mL) and collagenase type I (3 mg/mL) for 1 h under 37 °C. The digested solution was then filtrated, and the collected cells were seeded and cultured in Dulbecco's modified Eagle's medium (DMEM, Gibco, USA) containing 20% mesenchymal cell growth supplement (Lonza, USA) and antibiotics including100 U/mL penicillin, 100 mg/mL streptomycin and 0.25 mg/mL amphotericin B (Gibco, USA) under 37 °C with 5% CO_2. The cells were passaged every 3 days. For osteogenic differentiation, osteogenic differentiation culture medium (100 nM dexamethasone, 10 mM b-glycerophosphate and 200 mM ascorbate phosphate in DMEM) was used to culture PDLSCs.

### 2.2. Characterization of PDLSCs

After passaging for 3 times, PDLSCs were harvested and washed by PBS with 1% BSA three times. Then the cells were divided into several flow tubes and incubated with FITC conjugated antibodies of Stro-1 (NBP1-48356F), CD90 (FAB2067F), CD146 (NBP2-47777F), CD34 (NB600-1071F) and CD45 (NB110-81719) (Novus Biologicals, CO, USA) at room temperature for 45 min. After washing and suspension with 1% BSA/PBS, the signals were detected by flow cytometry. Alizarin red S (ARS) staining and alkaline phosphatase (ALP) staining were conducted by the kits in the guidance of the instructions (Nanjing Jiancheng, China).

2.3. Cell transfection

Negative control shRNA/siRNA and shRNA/siRNA against indicated gene were designed and ordered from GenePharma (Shanghai, China). Circ_0087960 cDNA or negative control cDNA
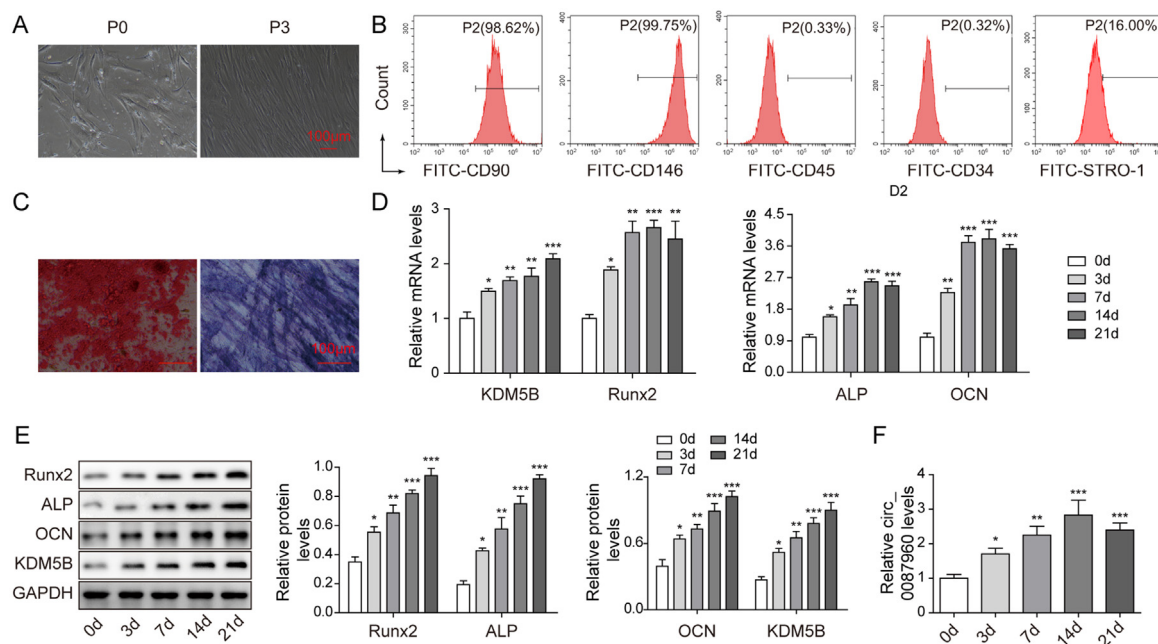
Fig. 1. Characterization and genes profile of PDLSCs. (A) Represented image of PDLSCs in the first passage and 3rd passage after isolation. (B) Flow cytometry results of PDLSCs for indicated surface markers. (C) Represented images of ALP and ARS staining of PDLSCs. (D) mRNA and (E) protein levels of indicated genes at different time points after osteogenic differentiation of PDLSCs. (F) Expression level of circ_0087960 at different time points after osteogenic induction of PDLSCs. n = 3, *$P < 0.05$, **$P < 0.01$, ***$P < 0.001$.
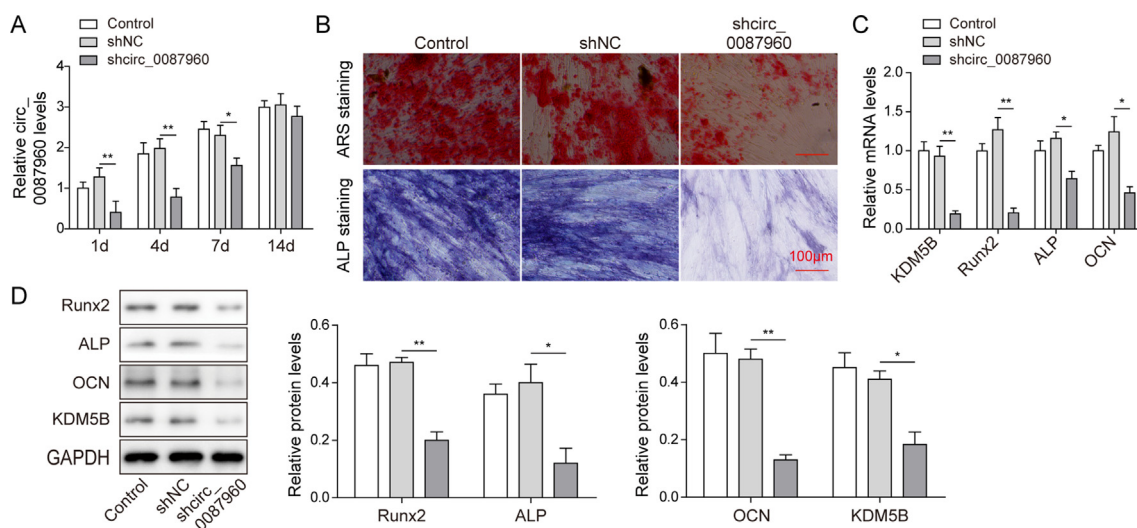
Fig. 2. Knocking down of circ_0087960 inhibited osteogenic differentiation. (A) Validation of circ_0087960 knocking down in PDLSCs at different time points post transfection. (B) Represented images of ALP and ARS staining of PDLSCs after indicated treatment. (C) mRNA and (D) protein levels of KDM5B, Runx2, ALP and OCN after indicated treatment. n = 3, *$P < 0.05$, **$P < 0.01$.

was amplified and cloned into the pcDNA3.1 expression vector. Lipofectamine 3000 (Invitrogen, CA, USA) was used for transfection with a 100 nM of shRNA/siRNA or cDNA plasmid according to the manufaturer's instructions.

2.4. Real-time quantitative PCR (RT-qPCR)

Total RNA was isolated by Trizol reagent (Invitrogen, USA) according to manufacturer's protocol. After quantification, and the reverse-transcription reactions were conducted with random primers and an M-MLV Reverse Transcriptase kit (Invitrogen, USA). RT-PCR was conducted using SYBR Green Supermixes (Cat. 1708882, Bio-Rad, USA). β-actin was used as internal control for normalization. Each sample was analyzed in triplicate. Relative expression of tested genes was normalized and analyzed by the $2^{-\Delta\Delta}$Ct method.

2.5. Western blot

Cells after indicated treatment were washed 3 times by cold PBS and dissolved with lysis buffer on ice for 20 min. After that, the cells were harvested, and after centrifugation, the supernatant containing the lysate was obtained and frozen under −80 °C. Protein qualities and concentrations were determined by the BCA assay kit (Cat. 5000001, Bio-Rad, USA). Protein samples were denatured and then separated by SDS-PAGE. The gels were then transferred into PVDF membranes (Cat. IPVH00010, Millipore, USA). After incubated with non-fat milk for 1 h, primary antibodies from Cell Signaling Technology (Danvers, USA) were used to incubate membranes under 4 °C overnight. Then the membranes were incubated with horseradish peroxidase (HRP)-conjugated secondary antibody for 1 h at room temperature. The proteins were visualized by an ECL reagent (Thermo Fisher Scientific). Primary mouse or rabbit monoclonal antibodies (diluted at 1:1000) against GAPDH (#5174), Runx2 (#8486), ALP (#8681), KDM5B (#15327), SKP2 (#2652), Flag-tag (#14793), Myc-tag (#2276) and HA-tag (#3724) were purchased from Cell Signaling Technology (MA, USA), and OCN

(ab93876) was purchased from Abcam (MA, USA). Secondary HRP-conjugated anti-mouse (#7076) or rabbit (#7074) IgG antibodies were purchased from Cell Signaling Technology (MA, USA) and used.

2.6. Co-immunoprecipitation (Co-IP) assay

Cells were dissolved in lysis buffer prepared as 25 mM Tris-HCl pH 7.4, 150 mM NaCl, 1 mM EDTA, 20 mM N-ethylmaleimide, 1% NP-40. 1000 μg of cell lysates were then added with primary antibody and incubated overnight. Then Protein A/G PLUS-Agarose (Santa Cruz, Sigma) was used adding into the samples and further incubated at 4 °C for 2 h, followed by washing with immunoprecipitation lysis buffer for 3 times. Then the protein samples were isolated and dissolved in 2X SDS sample buffer supplied with reducing agent and denatured by boiling. The harvested protein samples were then separated and detected by western blot. All Co-IP steps were performed at 4 °C unless otherwise indicated.

2.7. Electrophoretic mobility shift assay (EMSA)

Biotinylated probes were designed based on ChIP data and obtained from GenePharma (Shanghai, China). KDM5B protein was mixed with unlabeled probes or antibodies for 20 min at 4°, followed by the incubation with labeled probes for 20 min at room temperature. Free DNA or protein-DNA complex were separated in 6% polyacrylamide gels in tris-borate-EDTA for 2 h, then transferred into nylon membranes and visualized by streptavidin-HRP according to manufacturer's protocol (Thermo Fisher, USA).

2.8. RNA pulldown

For the assay of RNA pulldown, the Biotin RNA Labeling Mix (Roche Diagnostic, Indianapolis, USA) and T7 RNA polymerase (Roche) were used to synthesize RNAs labeled with biotin in vitro. Cell nuclear extraction (2 μg) was isolated and incubated with 100 pmol biotin-labeled RNAs. 100 μl of streptavidin agarose beads
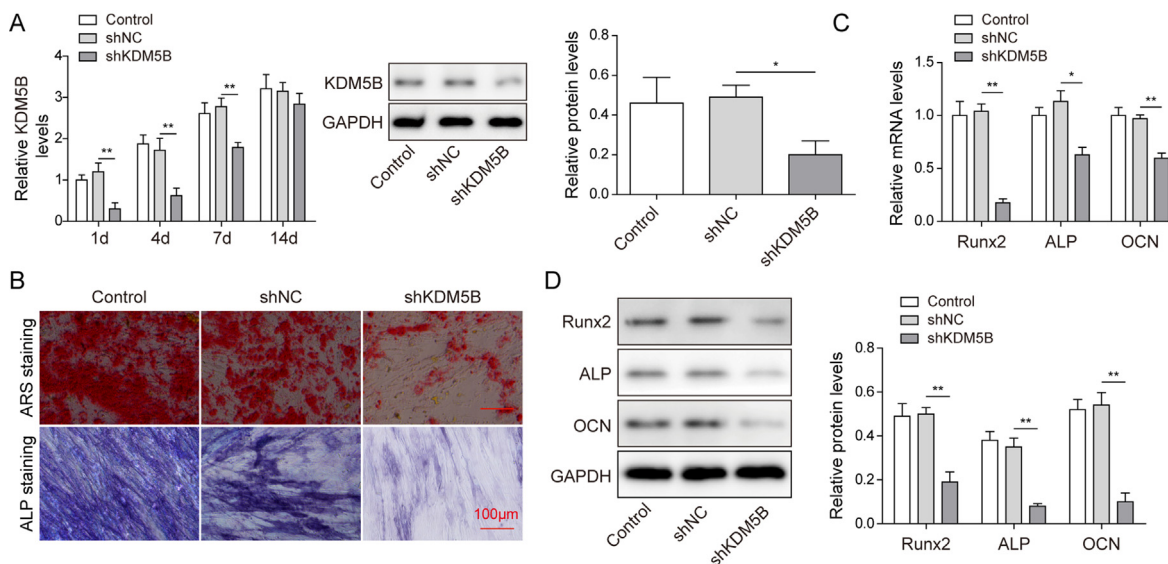
Fig. 3. Suppression of KDM5B inhibited osteogenic induction. (A) Validation of KDM5B inhibition by real-time PCR (at different time points post transfection) and western blot (4 days post transfection). (B) Images of ALP and ARS staining of PDLSCs after indicated treatment. (C) mRNA and (D) protein levels of KDM5B, Runx2, ALP and OCN after indicated treatment. n = 3, *$P < 0.05$, **$P < 0.01$.

were washed and added into each binding mixture, followed by incubation for 1 h under room temperature. After that, Beads were briefly washed for three times and then denatured by boiling in 2X SDS buffer, and the eluted protein samples were separated and detected by standard western blot technique.

2.9. Chromatin immunoprecipitation (ChIP) assay

ChIP assay was performed with the EZ-ChIP Kit (Millipore, USA) according to the manufacturer's instruction. PDLSCs chromatin was isolated and immunoprecipitated using anti-KDM5B antibody (Abcam, USA). Anti-IgG antibody (Abcam, USA) was used as a negative control. Calculation of fold enrichment as the ratio of KDM5B/IgG was determined by real-time PCR.

2.10. In vivo ubiquitination assay

293T cells were co-transfected with Flag-SFB-tagged KDM5B, Myc-tagged SKP2 and HA-tagged ubiquitin plasmids and after 24 h, cells were treated with MG132 for another 6 h. Cells were then lysed and boiled for 10 min, followed by sonication and dilution in IP buffer. Then the solution was immunoprecipitated with anti-Flag M2 affinity gel (Sigma, USA) at 4 °C. After overnight incubation, the beads were washed 5 times, 2X SDS loading buffer was used to elute the precipitated proteins, which were then applied to western blot with indicated antibodies.

2.11. Statistical analysis

All data are presented as mean ± standard deviation (SD) from at least three separate experiments. The differences between groups were determined using Student's t test or one-way ANOVA. The difference was deemed statistically significant at $P < 0.05$.

3. Results

3.1. Genes profiling of PDLSCs during osteogenic differentiation

Primary PDLSCs were isolated (P0) and passaged 3 times (P3) treated with osteogenic differentiation medium. Represented images of cell morphology were shown in Fig. 1A, exhibiting a spindle-like type for P3 cells. Several surface markers were detected by flowcytometry and as shown in Fig. 1B, Stro-1, CD90 and CD146, the mesenchymal stem cell markers, were highly expressed in P3 cells, while CD34 and CD45, the hematopoietic cell markers, were not detected. The osteogenic process evaluated by Alizarin Red S (ARS) staining and alkaline phosphatase (ALP) staining were shown in Fig. 1C, indicating an increased osteogenic activity.

Specifically, genes profiling of PDLSCs was conducted at different time points after differentiation (day 0, 3, 7, 14, and 21), especially for those have been reported to function in the PDLSCs differentiation. As shown in Fig. 1D and E, both mRNA and protein levels of KDM5B, Runx2, ALP and OCN were significantly increased in the differentiation period. Similar result was observed for circ_0087960 (Fig. 1F). Taken together, these results indicated that circ_0087960, KDM5B and osteogenic genes including ALP, Runx2 and OCN were upregulated during the osteogenic differentiation process of PDLSCs.

3.2. Knocking down of circ_0087960 inhibited osteogenic differentiation

To further explore the function of circ_0087960 in the process of osteogenic differentiation, we used shRNA to knock down its expression level in PDLSCs and validated at different time points as shown in Fig. 2A. Intriguingly, inhibition of circ_0087960 significantly suppressed the osteogenic differentiation compared to control treatment as presented by ARS staining (14 days post transfection) and ALP staining (7 days post transfection, Fig. 2B).
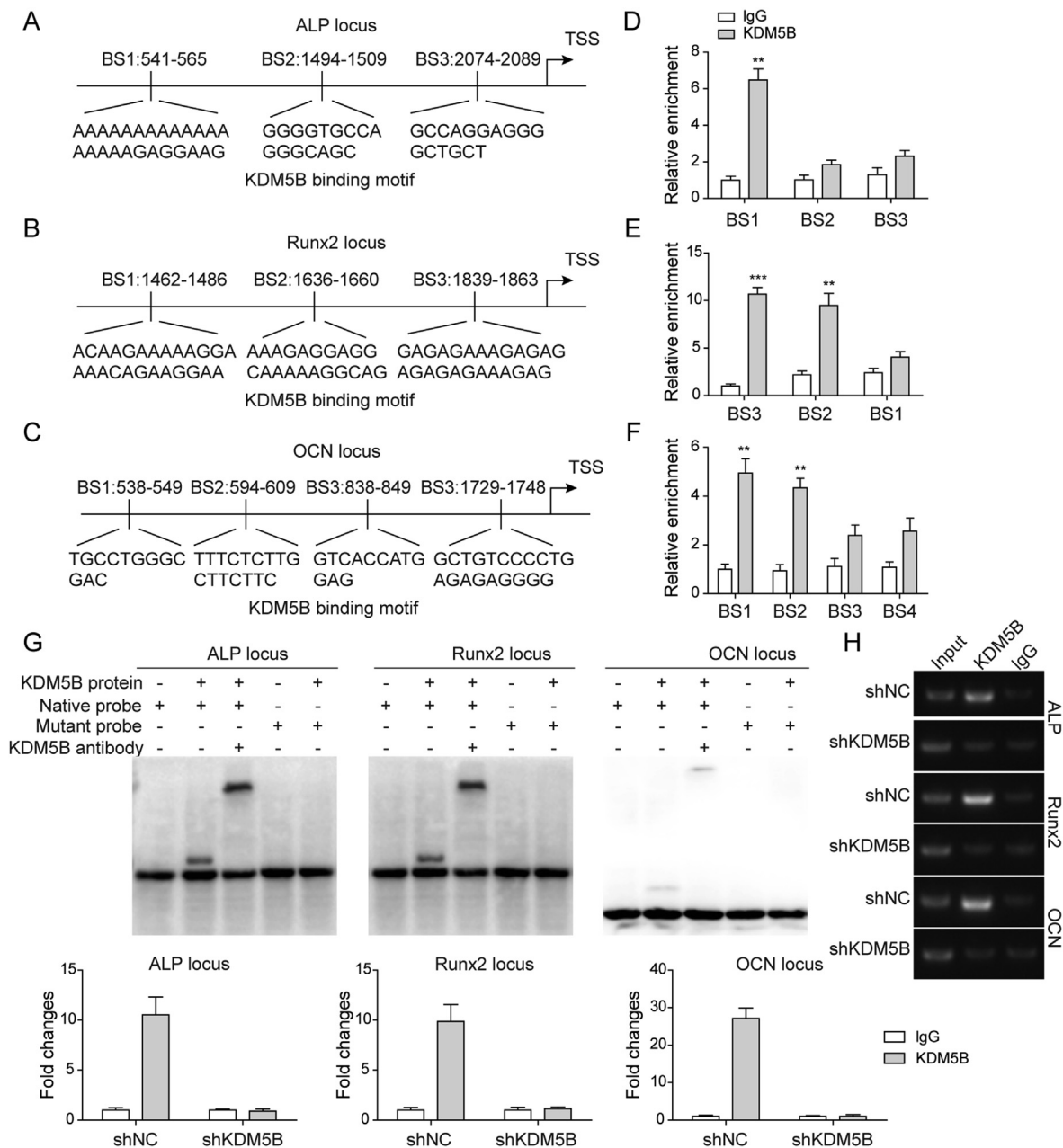
Fig. 4. KDM5B promoted osteogenic genes expression. (A–C) Illustration of predicted binding sites for KDM5B in the promoter regions of ALP, Runx2 and OCN gene locus. (D–F) Fold enrichment of ChIP assay in PDLSCs demonstrated the direct binding of KDM5B to indicated gene's promoter. (G) Representative images of EMSA assay showed the shift of indicated probes after incubation with KDM5B protein. (H) Representative images and statistic results showed the interaction of KDM5B and target genes promoters in PDLSCs by ChIP assay after transfection with scramble or KDM5B shRNA. n = 3, **$P < 0.01$, ***$P < 0.001$.

Meanwhile, the mRNA and protein levels of osteogenic genes Runx2, ALP and OCN were also detected 4 days after transfection and found to be dramatically downregulated upon circ_0087960 knockdown in PDLSCs (Fig. 2C and D).

3.3. Suppression of KDM5B inhibited osteogenic induction

Next, the potential function of KDM5B in osteogenic differentiation was also evaluated by shRNA knocking down in PDLSCs and validated at different time points for mRNA and 4 days post transfection for protein expression (Fig. 3A). Similarly, an inhibition of osteogenic differentiation was observed after KDM5B suppression compared to control group (Fig. 3B). Moreover, the expression

levels of Runx2, ALP and OCN were all remarkably decreased in PDLSCs in response to KDM5B knocking down (4 days post transfection, Fig. 3C and D). These data strongly suggested that circ_0087960 and KDM5B were involved in the process of osteogenic differentiation, which was inhibited upon their knocking down.

3.4. KDM5B regulated the expression of osteogenic related genes

As an important transcription factor, we speculated that KDM5B could regulate the expression of ALP, Runx2 and OCN from transcriptional level. At least three conserved binding motifs of KDM5B were identified in the upstream promoter regions of ALP, Runx2
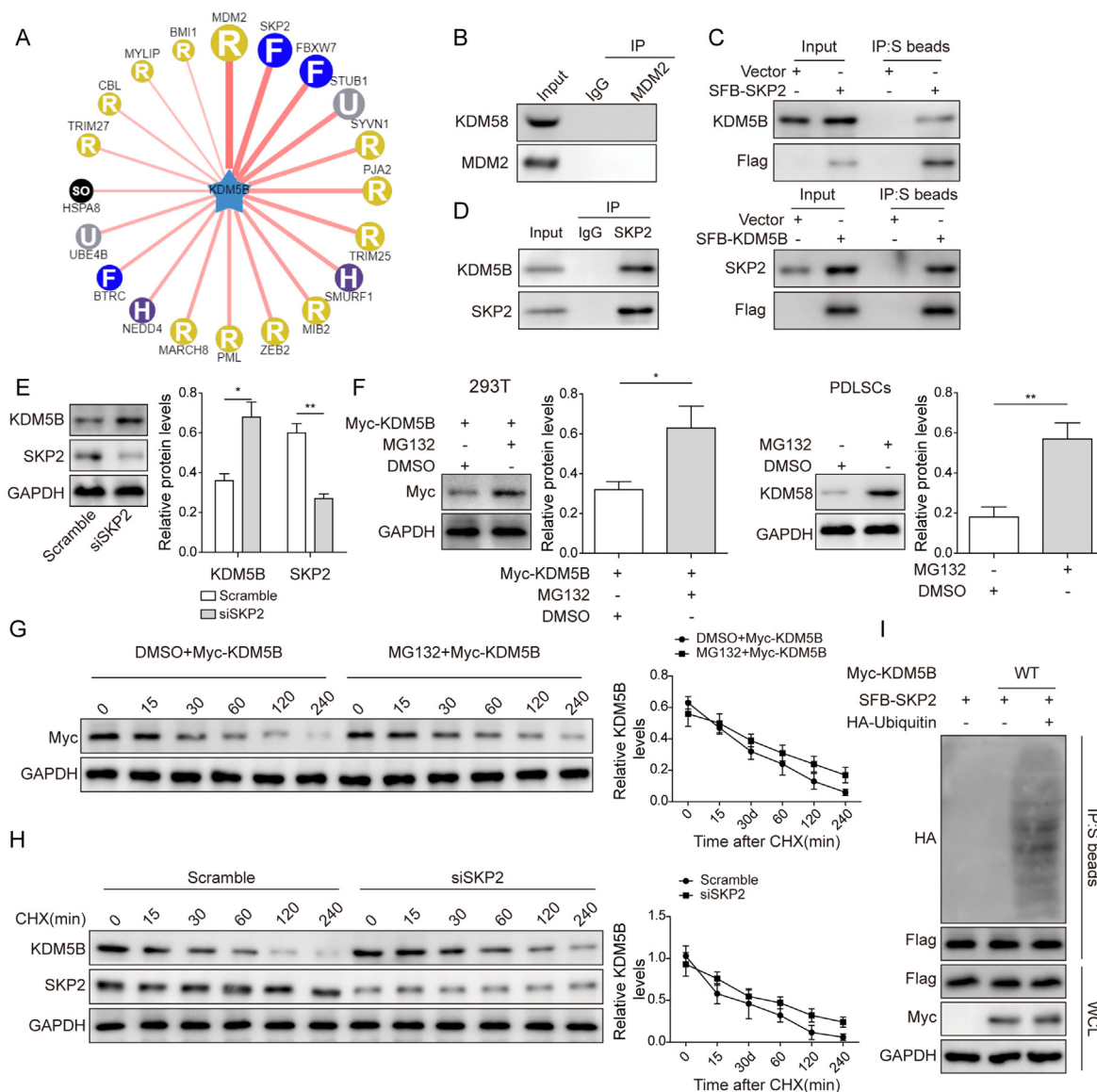
Fig. 5. SKP2 mediated ubiquitination and degradation of KDM5B in PDLSCs. (A) Prediction of recognition E3 ligases for KDM5B by UbiBrowser. (B) Co-IP validation indicated that KDM5B did not interact with MDM2 in PDLSCs. (C) Co-IP validation of exogenous expressed SKP2 and KDM5B in 293T cells. (D) Co-IP validation of endogenous interaction between SKP2 and KDM5B in PDLSCs. (E) Protein level of KDM5B in PDLSCs was upregulated 48 h after SKP2 inhibition. (F) The exogenous or endogenous KDM5B protein level was restored after MG132 treatment in 293T cells or PDLSCs. (G) The protein degradation test of exogenous KDM5B under indicated treatment in 293T cells. (H) The protein degradation test of endogenous KDM5B with SKP2 knocking down or scramble control in PDSCLs. (I) In vivo ubiquitination assay to determine the interaction between SKP2 and KDM5B. n = 3, *P < 0.05, **P < 0.01.

and OCN gene locus (Fig. 4A–C). ChIP assay was used to validate the interaction between KDM5B and predicated binding sites. As shown in Fig. 4D–F, the binding sites named as BS1(+541-+565) of ALP, BS2(+1636-+1660) and BS3 (+1839-+1863) of Runx2, and BS1 (+538-+549) and BS2(+594-+609) of OCN were found to be responsible for KDM5B interaction in PDLSCs. Furthermore, we utilized the EMSA assay to determine the direct binding of KDM5B and target genes' promoter. As shown in Fig. 4G, an obvious shift of wild-type probes of ALP, Runx2 and OCN promoter regions was observed in EMSA assay after incubation with KDM5B protein, while not the mutant ones. Meanwhile, the interaction of KDM5B and target genes promoters were inhibited when KDM5B was knocking down by shRNA in PDLSCs, which were demonstrated by ChIP assay (Fig. 4H). The above results demonstrated that KDM5B could regulate the expression of osteogenic genes via directly

binding to their promoter regions and enhancing their transcription and expression.

3.5. KDM5B was regulated and ubiquitinated by SKP2

The upstream regulator for KDM5B has not been clearly studied. Predicted ubiquitination site in KDM5B has been identified for E3 ligases SKP2 and MDM2 by UbiBrowser database (Fig. 5A). In our work, Co-IP assay was used to validation their interaction by exogenous expression of KDM5B and SKP2. As shown in Fig. 5B, KDM5B did not interact with MDM2 in PDLSCs. Meanwhile, SFB/Flag labeled SKP2 and KDM5B were transfected and overexpressed in 293T cell and direct interaction was demonstrated between KDM5B and SKP2 (Fig. 5C). Moreover, the endogenous interaction of these two proteins was further validated in PDLSCs by Co-IP
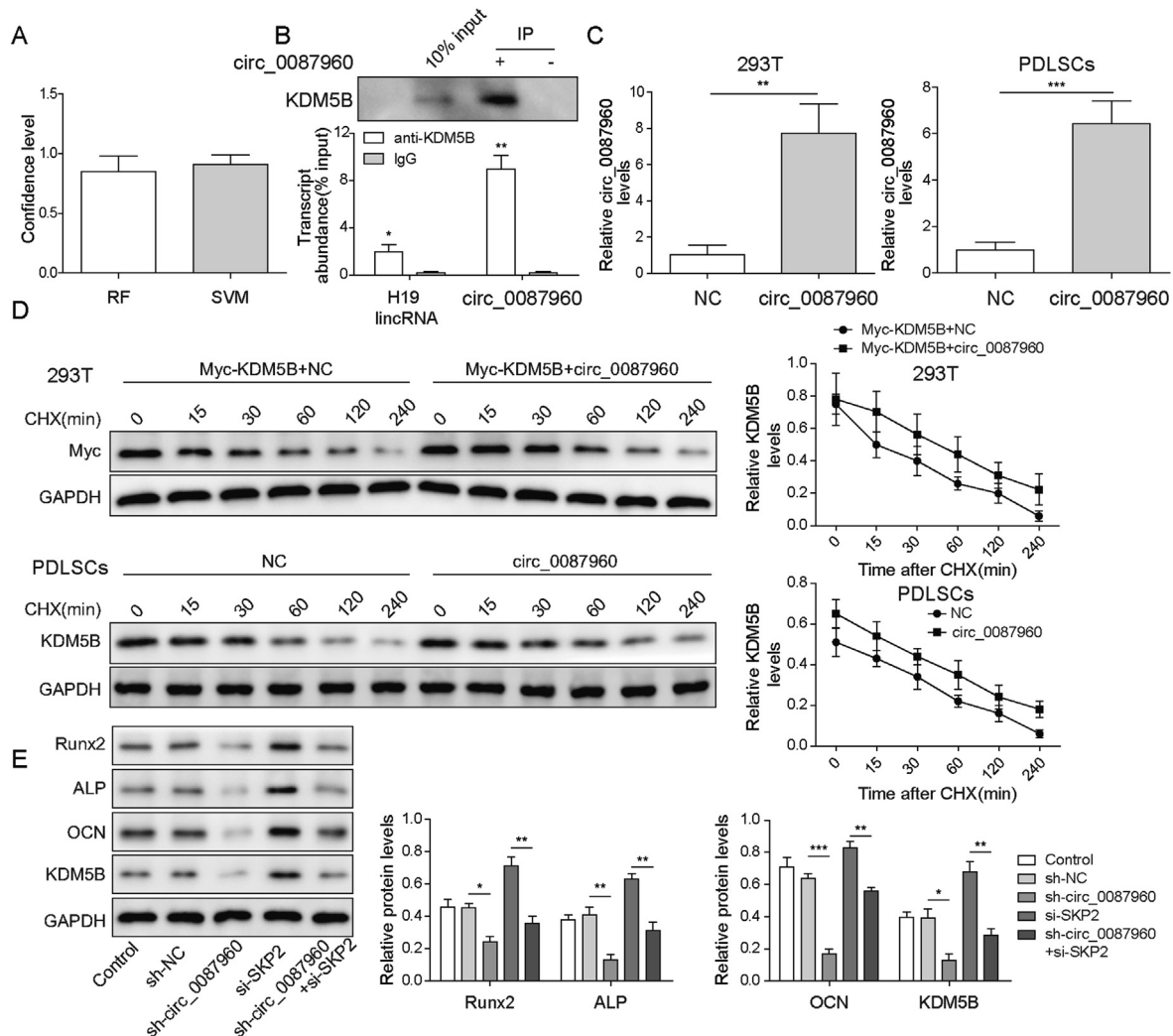
Fig. 6. Circ_0087960 bind to KDM5B and protected from SKP2-induced degradation. (A) Prediction of the interaction between circ_0087960 and KDM5B by RPIseq database. (B) RNA pull-down assay to determine the interaction between circ_0087960 and KDM5B, lncRNA H19 was used as a positive control. (C) Validation of circ_0087960 overexpression in 293T cells and PDLSCs. (D) Determination of KDM5B protein degradation after indicated treatment in 293T cells and PDLSCs. (E) Protein levels of KDM5B, ALP, Runx2 and OCN in PDLSCs after indicated treatment. n = 3, *$P < 0.05$, **$P < 0.01$, ***$P < 0.001$.

assay as shown in Fig. 5D. To explore if SKP2 could regulate KDM5B expression, we used siRNA against SKP2 to knock down its level in PDLSCs and found a significant upregulation of KDM5B protein level 48 h post transfection as shown in Fig. 5E. The proteinase inhibitor MG132 was used to treat 293T cells after overexpression of Myc-tagged KDM5B and it was found that blocking the protein degradation pathway could restore the level of KDM5B in 293T cells compared to DMSO treatment, and similar observation was achieved for the endogenous KDM5B in PDLSCs (Fig. 5F). Meanwhile, after blocking the protein synthesis by the treatment of protein synthesis inhibitor CHX, the degradation rate of KDM5B was tested and it was found that compared to DMSO treatment, MG132 treatment remarkably delayed the degradation rate of KDM5B in 293T cells (Fig. 5G). Of note, when SKP2 was inhibited by siRNA, the protein degradation of KDM5B was also significantly slowed down compared to control group, suggesting the involvement of SKP2 in the degradation of KDM5B (Fig. 5H). Since SKP2 is an E3 ubiquitin ligase for protein degradation, in vivo ubiquitination assay was performed to explore whether SKP2 affected KDM5B though ubiquitin-mediated degradation. 293T cells were co-transfected with SKP2, KDM5B and HA-tagged ubiquitin plasmids.

Surprisingly, KDM5B was found to be conjugated via ubiquitin in the presence of SKP2 as shown in Fig. 5I. Overall, these data indicated that KDM5B was regulated through SKP2-mediated ubiquitination in cells.

3.6. Circ_0087960 could protect KDM5B against ubiquitination and stimulate osteogenic genes expression

Circ_0087960 has been predicted to bind to the KDM5B protein by RPIseq database (Fig. 6A). In order to validate this hypothesis, we performed RNA pull-down assay in PDLSCs and found that circ_0087960 directly bind to KDM5B protein as shown in Fig. 6B, lncRNA H9 was used as a positive control for KDM5B binding. To further determine if circ_0087960 could affect the expression of KDM5B, it was transfected into 293T cells together with the Myc-tagged KDM5B or PDLSCs as shown in Fig. 6C. Surprisingly, the overexpressed circ_0087960 was able to slow down the degradation rate of both exogenous KDM5B protein in 293T cells and endogenous KDM5B in PDLSCs after CHX treatment compared to negative control group (Fig. 6D). Furthermore, the expression levels of KDM5B and its downstream targets were detected upon the

inhibition of circ_0087960 and SKP2 in PDLSCs. As shown in Fig. 6E, downregulation of circ_0087960 significantly repressed the expression of KDM5B, ALP, Runx2 and OCN, all of which were upregulated when SKP2 was knocking down. Intriguingly, the decreased levels of KDM5B, ALP, Runx2 and OCN induced by circ_0087960 shRNA were obviously rescued by the combination of SKP2 inhibition. These data strongly demonstrated that circ_0087960 could interact with KDM5B protein, protecting it from SKP2-mediated ubiquitination and degradation and enhancing the expression of osteogenic genes.

4. Discussion

Despite of the important functions of circRNAs in multiple cellular processes, very limited studies have been made about circRNAs in osteogenic differentiation. Circ_0087960, also named as circ_LPAR1, has been strongly confirmed of significant upregulation after osteogenic induction of PDLSCs for 5 and 7 days [11]. The hypothesized function of circ_0087960 is acting as a competing endogenous RNA (ceRNA) for miRNAs, regulating the downstream targets. However, no further evidence has been explored to support this hypothesis. In our work, consistent with the reported result, circ_0087960 was found to be stimulated upon the osteogenic differentiation of PDLSCs. More importantly, knocking down of circ_0087960 inhibited the osteogenic induction, as well as related genes expression, suggesting a significant role of circ_0087960 in the osteogenic differentiation of PDLSCs.

To further investigate the mechanism of how circ_0087960 affecting PDLSCs differentiation, we identified KDM5B as a potential partner for circ_0087960 because of the predicted binding in KDM5B protein. The histone demethylases KDM4B and KDM6B has been demonstrated to promote osteogenic differentiation of human MSCs [17], indicating the contribution and role of demethylases capability in osteoblast lineage commitment. Runx2 is a transcription factor that essential for bone development by modulating the expression of key target genes in differentiating osteoblastic cells [18]. Its transcription in osteoblast is controlled by regulatory elements within the P1 promoter region that recognized by other transcription factors during osteogenesis [19—22]. Recently, KDM5B has been shown to regulate the expression of Runx2 via epigenetic modulation of the P1 region in the osteogenic differentiation process [15]. Consistently, in our study, KDM5B was found to be upregulated after osteogenic induction and knocking down of KDM5B significantly caused the repression of Runx2, together with ALP and OCN. Specifically, several binding sites in the promoter regions of Runx2, ALP and OCN for KDM5B were identified and validated, providing the evidence for KDM5B-induced expression of osteogenic genes.

Besides the mechanism and downstream targets for KDM5B, we also explored the upstream regulator mediating KDM5B level during osteogenic induction. Previous study has proved that SKP2-mediated ubiquitination and protein degradation plays an important role in modulating KDM5B expression [16]. In our osteogenic differentiation system of PDLSCs, the same interaction was also verified and knocking down of SKP2 strongly delayed the degradation rate of KDM5B protein. Meanwhile, KDM5B was also validated to bind with circ_0087960 in PDLSCs, which in turn blocked the protein ubiquitination and enhanced the protein stability. Our results for the first time demonstrated that circ_0087960 could interact with KDM5B and protect it from SKP2-induced protein degradation, leading to an upregulation of KDM5B's downstream targets including Runx2, ALP and OCN and facilitating the osteogenic differentiation process.

In sum, our study identified circ_0087960 and KDM5B as positive regulators for osteogenic induction of PDLSCs by enhancing the expression of Runx2, ALP and OCN. Circ_0087960 was found to directly bind to KDM5B protein and block its interaction with SKP2, which could cause protein ubiquitination and degradation of KDM5B. The circ_0087960/KDM5B interaction amplified and facilitated the osteogenic differentiation, highlighting a promising therapeutic target for the application of PDLSCs in the treatment of periodontitis.

Ethics approval and consent to participate

The work was reviewed and permitted by the Medical Ethics Committee of Department of Stomatology, The Second Xiangya Hospital of Central South University. All the dental tissues used in this study were from patients signed the informed consent and underwent oral surgeries at the Department of Stomatology, The Second Xiangya Hospital of Central South University hospital.

Funding

Not applicable.

Declaration of competing interest

The authors declare that they have no known competing financial interests or personal relationships that could have appeared to influence the work reported in this paper.

Acknowledgements

We would like to give our sincere gratitude to the reviewers for their constructive comments.

Appendix A. Supplementary data

Supplementary data to this article can be found online at https://doi.org/10.1016/j.reth.2022.01.003.

References

[1] Reich E, Hiller KA. Reasons for tooth extraction in the western states of Germany. Community Dent Oral Epidemiol 1993;21(6):379—83.
[2] Xue P, Li B, An Y, Sun J, He X, Hou R, et al. Decreased MORF leads to prolonged endoplasmic reticulum stress in periodontitis-associated chronic inflammation. Cell Death Differ 2016;23(11):1862—72.
[3] Nancarrow-Lei R, Mafi P, Mafi R, Khan W. A systemic review of adult mesenchymal stem cell sources and their multilineage differentiation potential relevant to musculoskeletal tissue repair and regeneration. Curr Stem Cell Res Ther 2017;12(8):601—10.
[4] Trubiani O, Pizzicannella J, Caputi S, Marchisio M, Mazzon E, Paganelli R, et al. Periodontal ligament stem cells: current knowledge and future perspectives. Stem Cells Dev 2019;28(15):995—1003.
[5] Liu J, Zhao Z, Ruan J, Weir MD, Ma T, Ren K, et al. Stem cells in the periodontal ligament differentiated into osteogenic, fibrogenic and cementogenic lineages for the regeneration of the periodontal complex. J Dent 2020;92:103259.
[6] Onizuka S, Iwata T. Application of periodontal ligament-derived multipotent mesenchymal stromal cell sheets for periodontal regeneration. Int J Mol Sci 2019;20(11).
[7] Guo M, Qiu J, Shen F, Wang S, Yu J, Zuo H, et al. Comprehensive analysis of circular RNA profiles in skeletal muscles of aging mice and after aerobic exercise intervention. Aging (Albany NY) 2020;12(6):5071—90.
[8] Qu S, Yang X, Li X, Wang J, Gao Y, Shang R, et al. Circular RNA: a new star of noncoding RNAs. Cancer Lett 2015;365(2):141—8.
[9] Zhang C, Zhang B, Yuan B, Chen C, Zhou Y, Zhang Y, et al. RNA-Seq profiling of circular RNAs in human small cell lung cancer. Epigenomics 2020;12(8):685—700.
[10] Li X, Zheng Y, Zheng Y, Huang Y, Zhang Y, Jia L, et al. Circular RNA CDR1as regulates osteoblastic differentiation of periodontal ligament stem cells via the miR-7/GDF5/SMAD and p38 MAPK signaling pathway. Stem Cell Res Ther 2018;9(1):232.
[11] Xie X, Chen J, Ren X, Zhang M, Thuaksuban N, Nuntanaranont T, et al. Alteration of circRNA and lncRNA expression profile in exosomes derived from periodontal ligament stem cells undergoing osteogenic differentiation. Arch Oral Biol 2021;121:104984.

[12] Secombe J, Li L, Carlos L, Eisenman RN. The Trithorax group protein Lid is a trimethyl histone H3K4 demethylase required for dMyc-induced cell growth. Genes Dev 2007;21(5):537—51.

[13] Banck MS, Li S, Nishio H, Wang C, Beutler AS, Walsh MJ. The ZNF217 oncogene is a candidate organizer of repressive histone modifiers. Epigenetics 2009;4(2):100—6.

[14] Barrett A, Santangelo S, Tan K, Catchpole S, Roberts K, Spencer-Dene B, et al. Breast cancer associated transcriptional repressor PLU-1/JARID1B interacts directly with histone deacetylases. Int J Cancer 2007;121(2):265—75.

[15] Rojas A, Aguilar R, Henriquez B, Lian JB, Stein JL, Stein GS, et al. Epigenetic control of the bone-master Runx2 gene during osteoblast-lineage commitment by the histone demethylase JARID1B/KDM5B. J Biol Chem 2015;290(47): 28329—42.

[16] Lu W, Liu S, Li B, Xie Y, Adhiambo C, Yang Q, et al. SKP2 inactivation suppresses prostate tumorigenesis by mediating JARID1B ubiquitination. Oncotarget 2015;6(2):771—88.

[17] Ye L, Fan Z, Yu B, Chang J, Al Hezaimi K, Zhou X, et al. Histone demethylases KDM4B and KDM6B promotes osteogenic differentiation of human MSCs. Cell Stem Cell 2012;11(1):50—61.

[18] Stein GS, Lian JB, van Wijnen AJ, Stein JL, Montecino M, Javed A, et al. Runx2 control of organization, assembly and activity of the regulatory machinery for skeletal gene expression. Oncogene 2004;23(24):4315—29.

[19] Drissi H, Luc Q, Shakoori R, Chuva De Sousa Lopes S, Choi JY, Terry A, et al. Transcriptional autoregulation of the bone related CBFA1/RUNX2 gene. J Cell Physiol 2000;184(3):341—50.

[20] Henriquez B, Hepp M, Merino P, Sepulveda H, van Wijnen AJ, Lian JB, et al. C/EBPbeta binds the P1 promoter of the Runx2 gene and up-regulates Runx2 transcription in osteoblastic cells. J Cell Physiol 2011;226(11):3043—52.

[21] Lengner CJ, Hassan MQ, Serra RW, Lepper C, van Wijnen AJ, Stein JL, et al. Nkx3.2-mediated repression of Runx2 promotes chondrogenic differentiation. J Biol Chem 2005;280(16):15872—9.

[22] Zambotti A, Makhluf H, Shen J, Ducy P. Characterization of an osteoblast-specific enhancer element in the CBFA1 gene. J Biol Chem 2002;277(44): 41497—506.